Complete population inversion of maximally entangled states in 2^{2N}-level systems via Pythagorean-triple coupling

Muhammad Erew,* Moshe Goldstein,† and Haim Suchowski‡
Raymond and Beverly Sackler School of Physics and Astronomy, Tel Aviv University, Tel Aviv 6997801, Israel

(Received 5 January 2020; revised 18 January 2021; accepted 14 May 2021; published 31 August 2021)

Maximally entangled states play a central role in quantum information processing. Despite much progress throughout the years, robust protocols for manipulations of such states in many-level systems are still scarce. Here we present a control scheme that allows efficient manipulation of complete population inversion between two maximally entangled states. Exploiting the self-duality of SU(2), we present in this work a family of 2^{2N}-level systems with couplings related to Pythagorean triples that make a complete population inversion from one state to another (orthogonal) state, using very few couplings and generators. We relate our method to the recently developed retrograde-canon scheme and derive a more general complete transfer recipe. We also discuss the cases of $(2n)^2$-level systems, $(2n+1)^2$-level systems, and other unitary groups, and give a geometrical description of the inversion via the Majorana sphere.

DOI: 10.1103/PhysRevA.104.022616

I. INTRODUCTION

Quantum coherent control currently attracts a great deal of experimental and theoretical interest, especially toward multistate quantum systems [1–5]. Complete population inversion (CPI) plays an indispensable role in this effort [4,6–12], making it highly desirable to introduce novel efficient methods and models for building such transfer themes. For general time-dependent coupled dynamical equations, it is not easy to find solutions analytically. Even for a simple two level system there is a limited number of known time-dependent Hamiltonians that can be solved analytically and give a CPI [13,14]. Of special importance in this respect are maximally entangled states, which play a central role in quantum information processing. Despite much progress throughout the years, robust protocols for manipulations of such states in many-level systems are still scarce. Thus, controlled manipulation between such states and specifically CPI are naturally desirable.

Theoretical methods have been found and developed for complete controllability of systems [15,16]. However, these methods are nonconstructive and do not help in a concrete system. Due to the difficulty of synthesis and analysis of CPI schemes increases in multistate systems, multistate control problems are usually reduced to two-state ones [17–21]. Several approaches have been also proposed for CPIs in multilevel systems [22–27]. Recently, the dynamics of a four-level atomic system has been explored from a geometrical point of view, revealing that one can obtain CPIs in the laboratory frame if and only if some constraints on the couplings are obeyed [28]. In the case of periodic nearest-state coupling, the requirements of CPI were found to be linked to primitive Pythagorean triples [28]. Later on, the Pythagorean coupling scheme was verified experimentally in the realm of a four-level superconducting Josephson circuit [29].

In this work, using the self-duality of SU(2), we derive a general scheme for CPIs in 2^{2N}-level systems. We show that the basis for the CPI is composed of maximally entangled states. This observation is crucial for entangled-state manipulation, and we expect it to serve as a building block for future efficient quantum information processing protocols. It turns out that our is a generalization of the Pythagorean-triple coupling scheme [28] to higher representations of SU(2), offering a group-theoretical perspective on CPIs. We discuss the case of more general $(2n)^2$-level systems, relating our method to the recently developed retrograde canon scheme [30]. We also explain why our method does not apply to either $(2n+1)^2$-level or to higher unitary groups, but derive a general CPI recipe for general multistate systems. At the end we show how we can visualize the CPI on the Majorana sphere. Our scheme employs a substantially reduced number of couplings, allowing enormous simplification of its experimental realization in maximally entangled state control in various fields, including laser induced finite level systems [31], Josephson junctions [29], and waveguide arrays [32].

II. THE PYTHAGOREAN COUPLING AGAIN: THE DIAMOND FOUR-LEVEL SYSTEMS

In our current derivation, we reintroduce the Pythagorean coupling found in Ref. [28] from a different angle, which would allow its significant extension later on. We work with the two spin-$\frac{1}{2}$ Hamiltonians

$$h_{2\times 2}^{(1)} = \Delta_1\sigma_z + \Omega_1\sigma_x, \tag{1a}$$

$$h_{2\times 2}^{(2)} = \Delta_2\sigma_z + \Omega_2\sigma_x, \tag{1b}$$

where $\Delta_1, \Omega_1, \Delta_2, \Omega_2$ are nonzero real numbers. Ω_1 and Ω_2 represent real Rabi frequencies, and Δ_1 and Δ_2 represent the

*erew@tauex.tau.ac.il
†mgoldstein@tauex.tau.ac.il; http://www3.tau.ac.il/mgoldstein/index.php
‡haimsu@post.tau.ac.il; https://m.tau.ac.il/~haimsu/Home.html

 ©2021 American Physical Society

detunings. We construct the 4×4 Hamiltonian H,

$$H = h^{(1)} \oplus h^{(2)} = h^{(1)}_{2\times2} \otimes I^{(2)}_{2\times2} + I^{(1)}_{2\times2} \otimes h^{(2)}_{2\times2}, \tag{2}$$

and we denote this frame the tensor product (TP) frame.

With proper basis change, we obtain a laboratory-frame picture with nearest neighbor coupling that can be realized physically by a laser-field-driven four-level atom. This could be done by the orthogonal symmetric transformation matrix W composed of maximally entangled states (of which the von Neumann entropy is $\ln n$, where n is the dimension of the Hilbert space [4], and here it is 2):

$$W = \frac{1}{\sqrt{2}}(V(\Sigma_0), V(\Sigma_1), V(\Sigma_2), V(\Sigma_3)), \tag{3}$$

where the $V(\cdot)$ denotes the vectorization function described in Appendix A, and $\Sigma_0 = \sigma_0$, $\Sigma_1 = \sigma_1$, $\Sigma_2 = -i\sigma_2$, $\Sigma_3 = \sigma_3$ (σ_0 is the 2×2 unit matrix, and $\sigma_1, \sigma_2, \sigma_3$ are the Pauli matrices). A very useful property of this operator is $V(AXB) = (B^T \otimes A)V(X)$, and we use it frequently in this paper.

The Hamiltonian in the two frames is

$$H_{TP} = \begin{pmatrix} V_{14} & \Omega_2 & \Omega_1 & 0 \\ \Omega_2 & V_{23} & 0 & \Omega_1 \\ \Omega_1 & 0 & -V_{23} & \Omega_2 \\ 0 & \Omega_1 & \Omega_2 & -V_{14} \end{pmatrix}, \tag{4}$$

$$H_{\text{Lab}} = \begin{pmatrix} 0 & V_{12} & 0 & V_{14} \\ V_{12} & 0 & V_{23} & 0 \\ 0 & V_{23} & 0 & V_{34} \\ V_{14} & 0 & V_{34} & 0 \end{pmatrix}, \tag{5}$$

where $V_{12}, V_{23}, V_{34}, V_{14}$ are defined as follows:

$$\begin{pmatrix} V_{12} & V_{23} \\ V_{34} & V_{14} \end{pmatrix} = \begin{pmatrix} \Omega_1 + \Omega_2 & \Delta_1 - \Delta_2 \\ -\Omega_1 + \Omega_2 & \Delta_1 + \Delta_2 \end{pmatrix}. \tag{6}$$

Now, the dynamics described by the Schrödinger equation $\frac{\partial\psi}{\partial t} = -iH\psi$ lead to the unitary time-evolution operator (propagator) $U_{TP} = u^{(1)} \otimes u^{(2)} = e^{-ih^{(1)}t} \otimes e^{-ih^{(2)}t}$ (and $U_{\text{Lab}} = WU_{TP}W$). We are interested in CPIs between basis states in the laboratory frame. Let e_i denote the 4×1 matrix (column vector) which is zero everywhere except the ith component, which is 1 [in other words $(e_i)_{j1} = \delta_{ij}$]. Performing the calculation, one can see that, starting from e_1, one can fully transfer into e_3 if and only if

$$\begin{aligned} \Delta_1 &= \frac{1}{2}\frac{k(c-a)+b}{\sqrt{1+k^2}}, \quad \Omega_1 = \frac{1}{2}\frac{c-a-kb}{\sqrt{1+k^2}}, \\ \Delta_2 &= \frac{1}{2}\frac{k(c+a)-b}{\sqrt{1+k^2}}, \quad \Omega_2 = \frac{1}{2}\frac{c+a+kb}{\sqrt{1+k^2}}, \\ \tau &= \frac{\pi}{\sqrt{2c}}, \end{aligned} \tag{7}$$

where τ is the CPI time, k is an arbitrary real number, and $(a, b, c) = (\frac{p^2-q^2}{2}, pq, \frac{p^2+q^2}{2})$ where p and q are odd integers ($p > q$). We see that the triple (a, b, c) has the the well-known general form of a Pythagorean triple, and it is called primitive when p and q are coprime, $\gcd(p, q) = 1$. Notice that not just primitive Pythagorean triples (PPTs) give solutions, but also nonprimitive ones. However, Hamiltonians generated from triples that are not primitive are simply Hamiltonians that are generated from PPTs multiplied by an odd integer constant.

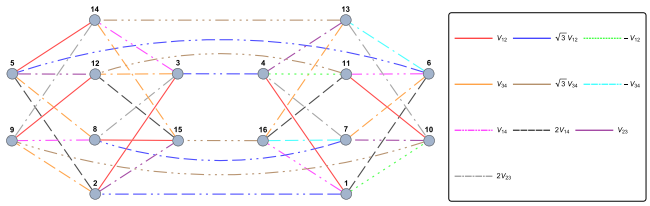

FIG. 1. The couplings of the 16-level system. A CPI occurs between level 1 and level 13. One can see that the coupling structure requires much less independent couplings than a general 16-level system, which will allow a simplified experimental realization.

So we can restrict ourselves just to PPTs. On the other hand, taking negative numbers, like $(a, b, c) = (-\frac{p^2-q^2}{2}, pq, \frac{p^2+q^2}{2})$ for example, suggests new inequivalent Hamiltonians, so those should be included as well.

III. GENERALIZING TO OTHER REPRESENTATIONS

The way we developed the scheme of CPI suggests a natural generalization to other representations of $\mathfrak{su}(2)$. Motivated by the fact that the Lie algebra structure is more fundamental than its representation, we investigate the CPI condition for higher dimensional representations of $\mathfrak{su}(2)$. So we consider now the Hamiltonian

$$h^{(1)}_{n\times n} = 2\Delta_1 J^{(n)}_3 + 2\Omega_1 J^{(n)}_1 \tag{8a}$$

$$h^{(2)}_{n\times n} = 2\Delta_2 J^{(n)}_3 + 2\Omega_2 J^{(n)}_1 \tag{8b}$$

$$H = h^{(1)}_{n\times n} \otimes I^{(2)}_{n\times n} + I^{(1)}_{n\times n} \otimes h^{(2)}_{n\times n}, \tag{8c}$$

and we want to get a CPI in n-dimensional representations. Here the matrices $\{J^{(n)}_1, J^{(n)}_2, J^{(n)}_3\}$ are the known basis of the n-dimensional irreducible (spin-$\frac{n-1}{2}$) representation of $\mathfrak{su}(2)$. They satisfy $[J^{(n)}_i, J^{(n)}_j] = i\varepsilon_{ijk}J^{(n)}_k$, with real $J^{(n)}_1$, imaginary $J^{(n)}_2$, and diagonal $J^{(n)}_3$. We mention in passing that calculating the time evolution operator of such Hamiltonians becomes much easier when one uses the Cayley-Hamilton theorem [33,34].

The main challenge in the higher-dimensional case is finding a generalized matrix W which would give a laboratory frame Hamiltonian with a realistic structure and symmetry of its nonvanishing matrix elements (see for example Fig. 1). For $n = 2^N$, this could be achieved if one constructs W out of maximally entangled states. This W is composed of the vectorization of tensor products of N matrices from the set $\{\Sigma_0, \Sigma_1, \Sigma_2, \Sigma_3\}$ (with a normalization factor $\frac{1}{\sqrt{2^N}}$). The resulting vectors are automatically orthogonal, making W an orthogonal matrix. One can order them in a way that makes W symmetric as well. We can fix W by imposing the following demands: (a) the first n columns do not contain negative values, (b) the first half of the diagonal contains just positive values and the second just negative values, and (c) the last column contains alternating 1's and (−1)'s, in addition to zeros. This structure is a natural generalization of the 4×4 case presented above. In this laboratory frame, and because of our convention of building the rotational matrix, we always achieve a CPI from e_1 to e_{n^2-n+1}.

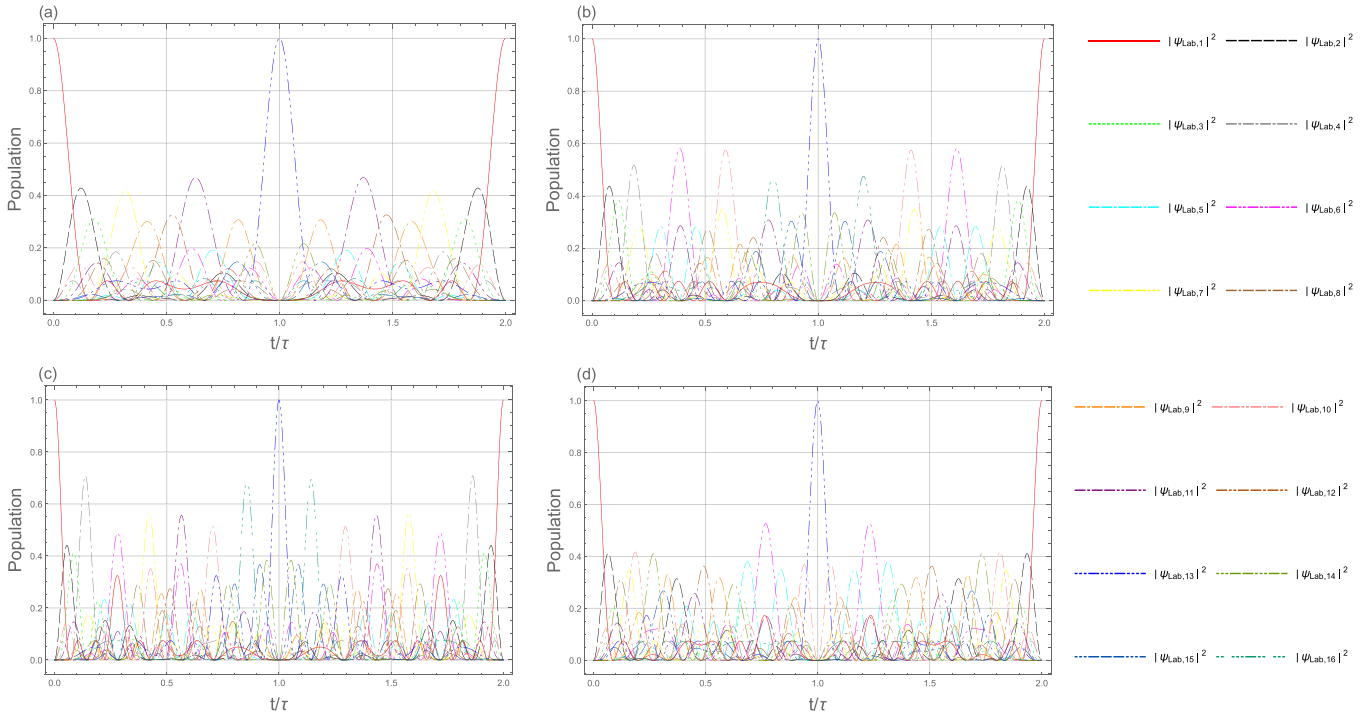

FIG. 2. The dynamics of Pythagorean 16-level systems: Numerical simulations of the CPI between $|1\rangle$ and $|13\rangle$ in the laboratory frame of the 16-level system are shown for different PPTs: (a) $p = 3, q = 1, k = 0 \to (a, b, c) = (4, 3, 5), k = 0$; (b) $p = 5, q = 1, k = 0 \to (a, b, c) = (12, 5, 13), k = 0$; (c) $p = 7, q = 1, k = 0 \to (a, b, c) = (24, 7, 25), k = 0$; (d) $p = 5, q = 3, k = 0 \to (a, b, c) = (8, 15, 17), k = 0$. The evolution of the population in each state is described as a function of time (measured in τ units) when the system is prepared in the ground state $|1\rangle$.

To simplify the expressions, let us denote the column vector $V(\bigotimes_{i=1}^{k} \Sigma_{n_i})$ by $\underline{n_1 n_2 \dots n_k}$, where $n_1, \dots, n_k$ can assume the values 0, 1, 2, and 3. For example, by $\underline{0031}$ we mean $V(\Sigma_0 \otimes \Sigma_0 \otimes \Sigma_3 \otimes \Sigma_1)$. With this notation, W for the case of $N = 1$ (which means that $n = 2$ and we work with a four-level system) is $W_{4\times4} = \frac{1}{\sqrt{2}}(\underline{0}, \underline{1}, \underline{2}, \underline{3})$ [see Eq. (3)].

In the language of the TP frame, the CPI we are talking about is always from the state proportional to $\underline{00\dots00}$ to the state proportional to $\underline{11\dots112}$ (Y_n always has 1's and (-1)'s alternately on the antidiagonal, and 0's elsewhere). In the case of $N = 1$ it is from $\underline{0}$ to $\underline{2}$ in the TP frame, which means it is from e_1 to e_3 in the laboratory frame.

As an example, when $N = 2$ (this means that $n = 4$ and we work with a 16-level system), one may use this orthogonal symmetric transformation to go to the laboratory frame:

$$W_{16\times16} = \tfrac{1}{2}(\underline{00}, \underline{01}, \underline{10}, \underline{11}, \underline{31}, \underline{30}, \underline{21}, \underline{20}, \underline{23}, \underline{22}, \underline{33}, \underline{32}, \underline{12}, \underline{13}, \underline{02}, \underline{03}). \tag{9}$$

The matrix is written out explicitly in Appendix B.

The TP frame Hamiltonian and the laboratory frame Hamiltonian are both presented in Appendix B. For simplicity, we illustrate the couplings in the laboratory frame by an undirected graph in Fig. 1. We can see also in Fig. 2 that numerical results confirm the periodic CPI between $|1\rangle$ and $|13\rangle$.

The rotation matrix for the case $N = 3$, which means that $n = 8$ and we work with a 64-level system, is presented in Appendix C.

It is important to realize that the fact that $V(I_n)$ goes to $V(e^{-i\pi J_2^{(n)}})$ in the TP frame through $U = u_1 \otimes u_2$ is nothing but a manifestation of the fact that we are working in different representations of the same group. The question to be asked is, Is this a CPI in every representation? In order for it to be a CPI in every representation, the two states must be orthogonal. It is trivial to understand that this holds when n is even, since $e^{-i\pi J_y}$ always has alternating 1's and (-1)'s on the antidiagonal, and 0's elsewhere.

So, for every even n we have this CPI from $\frac{1}{\sqrt{n}}V(I_n)$ to $\frac{1}{\sqrt{n}}V(e^{-i\pi J_2^{(n)}})$. Thus, any orthogonal rotation which has the two rows $\frac{1}{\sqrt{n}}V^T(I_n)$ and $\frac{1}{\sqrt{n}}V^T(e^{-i\pi J_2^{(n)}})$ would lead us to a frame in which we have a CPI there (between these two states). What is special in the $n = 2^N$ cases is that we can find there a laboratory frame in which the Hamiltonian has many symmetries that can be seen via coupling diagrams or coupling undirected graphs, and all of the states are maximally entangled states.

IV. THE QUANTUM RETROGRADE CANON POINT OF VIEW

We will now relate the CPI scheme we built to the quantum retrograde canon [30], investigate the retrograde canon for other unitary groups, and then give a more general CPI recipe.

In fact, the CPI we found here in higher dimensions is related to the retrograde canon procedure [30]. We will discuss it from a group theoretical perspective, which would allow its subsequent generalization to higher unitary groups. Here we give a one-direction claim, and from the reversibility of the proof we deduce that the other direction also holds. If $H(t)$ is

the Hamiltonian of a two level system, and its time evolution operator,

$$U(t,t_0)=\mathcal{T}\exp\left(-\frac{i}{\hbar}\int_{t_0}^{t}dt'H(t')\right), \tag{10}$$

satisfies

$$U(T,0)|\uparrow\rangle=|\downarrow\rangle \tag{11}$$

[from unitarity we immediately see that $U(T,0)=|\downarrow\rangle\langle\uparrow|-|\uparrow\rangle\langle\downarrow|=\Sigma_2$], then the Hamiltonian

$$\mathcal{H}(t)=-H(T-t)\otimes I+I\otimes H(t), \tag{12}$$

whose propagator is

$$\mathcal{U}(t,t_0)=U(T-t,T-t_0)\otimes U(t,t_0), \tag{13}$$

satisfies

$$\mathcal{U}\left(\frac{T}{2},0\right)V(I)=V(\Sigma_2). \tag{14}$$

The proof proceeds as follows: Since we know that $U(T,0)=\Sigma_2$ and Σ_2 satisfies $u\Sigma_2u^T=\Sigma_2$ for every $u\in$ SU(2), we can see that

$$U\left(\frac{T}{2},T\right)U(T,0)U^T\left(\frac{T}{2},T\right)=\Sigma_2. \tag{15}$$

And since the propagator satisfies $U(t_3,t_2)U(t_2,t_1)=U(t_3,t_1)$ (for every t_1,t_2,t_3) we get

$$U\left(\frac{T}{2},0\right)U^T\left(\frac{T}{2},T\right)=\Sigma_2, \tag{16}$$

and therefore (see Appendix A)

$$\begin{aligned}\mathcal{U}\left(\frac{T}{2},0\right)V(I)&=U\left(\frac{T}{2},T\right)\otimes U\left(\frac{T}{2},0\right)V(I)\\&=V\left(U\left(\frac{T}{2},0\right)IU^T\left(\frac{T}{2},T\right)\right)\\&=V(\Sigma_2).\end{aligned} \tag{17}$$

We can see in the proof that all the steps are reversible, so that the other direction holds. We can summarize:

$$U(T,0)|\uparrow\rangle=|\downarrow\rangle\Leftrightarrow\mathcal{U}\left(\frac{T}{2},0\right)V(I)=V(\Sigma_2); \tag{18}$$

and the Pythagorean Hamiltonian that we deal with can be obtained from this procedure [30]. Notice that $\Sigma_2=e^{-i\pi\frac{\sigma_2}{2}}=e^{-i\pi J_2^{(2)}}$, so we can extend our claim to other representations, by simply replacing Σ_2 by $Y_n=e^{-i\pi J_2^{(n)}}$.

A natural question arises: Can we claim a similar retrograde statement for the other unitary groups SU(n) (when $n>2$)? The answer is no; and the deep reason of this lies in the fact that the only group tht is self-dual (the dual of each irreducible representation is isomorphic to it) among these is just SU(2).

For every SU(n), $n\otimes\overline{n}=1\oplus(n^2-1)$, which means that there is a scalar state which does not change under $U\otimes\overline{U}$, which is of course the state proportional to $V(I)$, since $\overline{U}=U^*$. With this in mind we define first the semiretrograde Hamiltonian

$$\mathcal{H}(t)=H^*(T-t)\otimes I+I\otimes H(t) \tag{19}$$

whose propagator is

$$\mathcal{U}(t,t_0)=U^*(T-t,T-t_0)\otimes U(t,t_0), \tag{20}$$

and immediately conclude that

$$U(T,0)=I\iff\mathcal{U}\left(\frac{T}{2},0\right)V(I)=V(I), \tag{21}$$

where the proof is very similar to what we did in the retrograde canon's proof. However, this does not give a CPI recipe.

SU(2) is special since it is self-dual: Any irreducible representation of SU(2) is isomorphic to its dual representation. A representative example would be the simple representation called 2. $\overline{2}$ is isomorphic to 2 via the transformation $Y=e^{-i\frac{\pi}{2}\sigma_y}$. Only because of this unique feature of self-duality of SU(2) we could get our CPI from $V(I)$ to $V(Y)$.

In fact, for any SU(n), if we have two dual isomorphic representations (of the same dimension) ρ and ρ^*, where the isomorphism is the matrix $Y^\dagger$ (it has to be unitary), i.e.,

$$Y^\dagger\rho(g)Y=\rho^*(g)\ \ \forall g\in\mathrm{SU}(n), \tag{22}$$

we get $uYu^T=Y$ for every $u\in$ SU(n), and the same proof scheme holds here too. We get in this case

$$U(T,0)=Y\iff\mathcal{U}\left(\frac{T}{2},0\right)V(I)=V(Y). \tag{23}$$

where $U(t,t_0)$ and $\mathcal{U}(t,t_0)$ are defined as in Eqs. (10) and (13), and $H(t)\in\rho$. This is a CPI if and only if $\mathrm{tr}(Y)=0$, which is equivalent to orthogonality between $V(I)$ and $V(Y)$.

Although we could not get an analogous CPI procedure in other special unitary groups, we still can generate a similar argument for a general multistate Hamiltonian. It is not the same since it does not depend on a singlet state of a group, and it also deals with any quantum mechanical system. The similarity is for the states we use in this argument, and in the case of two-level systems it reduces to the retrograde canon we presented before. The statement goes as follows: For a general multistate Hamiltonian $H(t)$ whose propagator is $U(t,t_0)$ [Eq. (10)]: If there are two normalized states $|i\rangle$ and $|f\rangle$ such that

(1) $|\langle i\mid f\rangle|<1$,
(2) $U(T,0)|i\rangle=|f\rangle$, and
(3) $U(T,0)|f\rangle=e^{i\phi}|i\rangle$, where ϕ is real,

then [we define the retrograde Hamiltonian and its propagator as in Eqs. (12) and (13), and define the two states $|g\rangle\equiv U(\frac{T}{2},0)|i\rangle$ and $|h\rangle\equiv U(\frac{T}{2},0)|f\rangle$]

$$\begin{aligned}&\mathcal{U}\left(\frac{T}{2},0\right)(-e^{i\phi}|ii\rangle+|ff\rangle)\\&=U\left(\frac{T}{2},T\right)\otimes U\left(\frac{T}{2},0\right)(-e^{i\phi}|ii\rangle+|ff\rangle)\\&=U\left(\frac{T}{2},0\right)\otimes U\left(\frac{T}{2},0\right)(-|fi\rangle+|if\rangle)\\&=-|hg\rangle+|gh\rangle,\end{aligned} \tag{24}$$

and this is a CPI (normalization is needed of course).

If the Hamiltonian $H(t)$ is time independent, the conditions reduce to

(1) $U(2T)|i\rangle=e^{i\phi}|i\rangle$ and
(2) $|\langle i\mid U(T)\mid i\rangle|<1$,

and we get CPIs not just from $-e^{i\phi}|ii\rangle + |ff\rangle$, but also from $U(t)\otimes U(t)$ acting on $-e^{i\phi}|ii\rangle + |ff\rangle$ for every t (as an initial state). From the argument presented here we can understand that there are basic CPIs in our system, and from them we can build our universal CPI in any even-dimensional representation. We can also investigate the problem with odd-dimensional representations again from another point of view. For more details see Appendix D and Appendix E. Moreover, for the time-independent Hamiltonian case, we always can satisfy the two conditions if we start with a combination of two eigenstates (with two nonzero coefficients), and hence they are always fulfilled in two level systems. Other cases of multilevel systems and general time-dependent Hamiltonian may be investigated using the Poincaré recurrence theorem [35–38].

V. GEOMETRICAL REPRESENTATION: THE MAJORANA SPHERE FOR THE PYTHAGOREAN FOUR-LEVEL SYSTEM

The well-known geometric visualization of the Bloch sphere plays an important role in developing a clear intuitive understanding of two-level dynamics [39,40]. Here we expand the standard Bloch sphere geometrical visualization: We visualize the full "path" (of time evolution) of the system's state in the four-level Pythagorean system in both frames (the TP frame and the laboratory frame) on the the Majorana sphere (the extension of the Bloch sphere to higher dimensions; see Appendix F). Based on Majorana's decomposition, a state with angular momentum j can be thought of as fully symmetrized state of $2j$ spin-$\frac{1}{2}$ particles [41–43], and then represented as $2j$ points on the surface of the unit sphere [44]. When the system evolves in time, these points follow trajectories on the unit sphere. Another way of visualizing the dynamics is to depict the trajectory of the propagator evolution on the unit 3-ball (See [30]).

According to Majorana's representation, there is a one-to-one correspondence between the (normalized) states of an N-level system and the (normalized) $N-1$ Majorana polynomials, which in turn are uniquely determined by their roots. The number of roots can be up to $N-1$. Each root, which is a complex number, can be presented on the unit sphere $\mathcal{S}^2$ by using the stereographic projection from the south pole. Therefore, we can depict the state of the system by these points on the unit sphere, which we will refer to as the Majorana sphere.

Thus, in an N-level system, the time evolution on the Majorana sphere can be represented by $N-1$ trajectories (or less), where every trajectory describes the evolution of a root. Majorana's theorem states that, with an applied magnetic field on the system (which has angular momentum j, where $N=2j+1$ and $|k\rangle$ in our notation is $|j, m=k-j\rangle$), these representative points precess rigidly around the direction of the field. For more details see Appendix F. Here, in this section, we depict the trajectory itself of the state (its evolution in time) in our system (in which $N=4$ and $j=\frac{3}{2}$).

In the TP frame, we start with $|\psi\rangle = \frac{1}{\sqrt{2}}(|1\rangle + |4\rangle)$, which is represented by the three roots $z_1 = e^{-i\frac{2\pi}{3}}$, $z_2 = 1$, $z_3 = e^{i\frac{2\pi}{3}}$, and so by the three points $(\theta_1,\phi_1) = (\frac{\pi}{2}, -\frac{2\pi}{3})$, $(\theta_2,\phi_2) = (\frac{\pi}{2}, 0)$, $(\theta_3,\phi_3) = (\frac{\pi}{2}, \frac{2\pi}{3})$ on $\mathcal{S}^2$, and end with $|\psi\rangle \propto \frac{1}{\sqrt{2}}(|2\rangle - |3\rangle)$, which is represented by the two roots $z_1 = 0$, $z_2 = -1$, and so by the two points $(\theta_1,\phi_1) = (0,0)$, $(\theta_2,\phi_2) = (\frac{\pi}{2}, \pi)$ on $\mathcal{S}^2$. The trajectories are depicted in Fig. 3.

In the laboratory frame, we start with $|\psi\rangle = |1\rangle$, which is represented by the three identical roots $z_1 = 0$, $z_2 = 0$, $z_3 = 0$, and so by the three identical points $(\theta_1,\phi_1) = (0,0)$, $(\theta_2,\phi_2) = (0,0)$, $(\theta_3,\phi_3) = (0,0)$ on $\mathcal{S}^2$, and end with $|\psi\rangle \propto |3\rangle$, which is represented by the single root $z_1 = 0$, and so by the one point $(\theta_1,\phi_1) = (0,0)$ on $\mathcal{S}^2$. The trajectories are depicted in Fig. 3.

VI. CONCLUSION

We presented a way of manipulating maximally entangled states in 2^{2N}-level systems using a generalization of the Pythagorean-triples coupling scheme. For this we used a basis of maximally entangled states in which the Hamiltonian has a realistic structure and symmetry of its nonvanishing matrix elements, with a substantially reduced number of couplings, allowing enormous simplification of its experimental realization in maximally entangled state control. We would like to stress that this method gives complete population transfer schemes for many pairs of specific entangled states for the same system. It suggests many different Hamiltonians; each one of them gives rise to a complete population inversion between two specific maximally entangled states, and between pairs of (not maximally) entangled states.

We must clarify that the scheme does not necessarily refer to two physical subsystems. It deals with any system that has $2^{2N}\times 2^{2N}$ structure. This includes degenerate 2^{2N}-state systems that cannot be separated physically into two subsystems with no interaction but can still be decomposed mathematically. This structure is not just a mathematical curiosity, but applies to actual physical systems, as was done numerically with transitions in ^{85}Rb [28] and experimentally in a four-level Josephson circuit [29] for $N=1$. We strongly believe that there are other interesting physical systems with $N>1$ in which we can perform the scheme, such as a hydrogen-like atom, including Rydberg states, with degenerate energy subspaces [45], path-qudits in integrated photonics [46], etc. In the case of two physically separate subsystems, our discussion assumes starting from an entangled state, which can be created using established techniques, such as the Sørensen-Mølmer [47] protocol for ion chains. Our scheme then allows transfer between two maximally-entangled states without requiring further application of entangling gates.

Other $(2n)^2$-level systems do have the same CPI, but we could not build for them real laboratory Hamiltonians that had the same symmetries of the couplings. We found that this scheme, which is based on the quantum retrograde canon, is unique for SU(2) and gave a similar argument (which does not give a CPI by itself) for SU(n) where $n \geqslant 3$. In addition, we derived a more general CPI recipe for general multistate systems.

Other groups and schemes could be considered in a similar way in order to build schemes for them, if possible, but an immediate case of interest is the quaternionic (or pseudoscalar) representations of SU(n) which exist for $n=4k+2$. In this

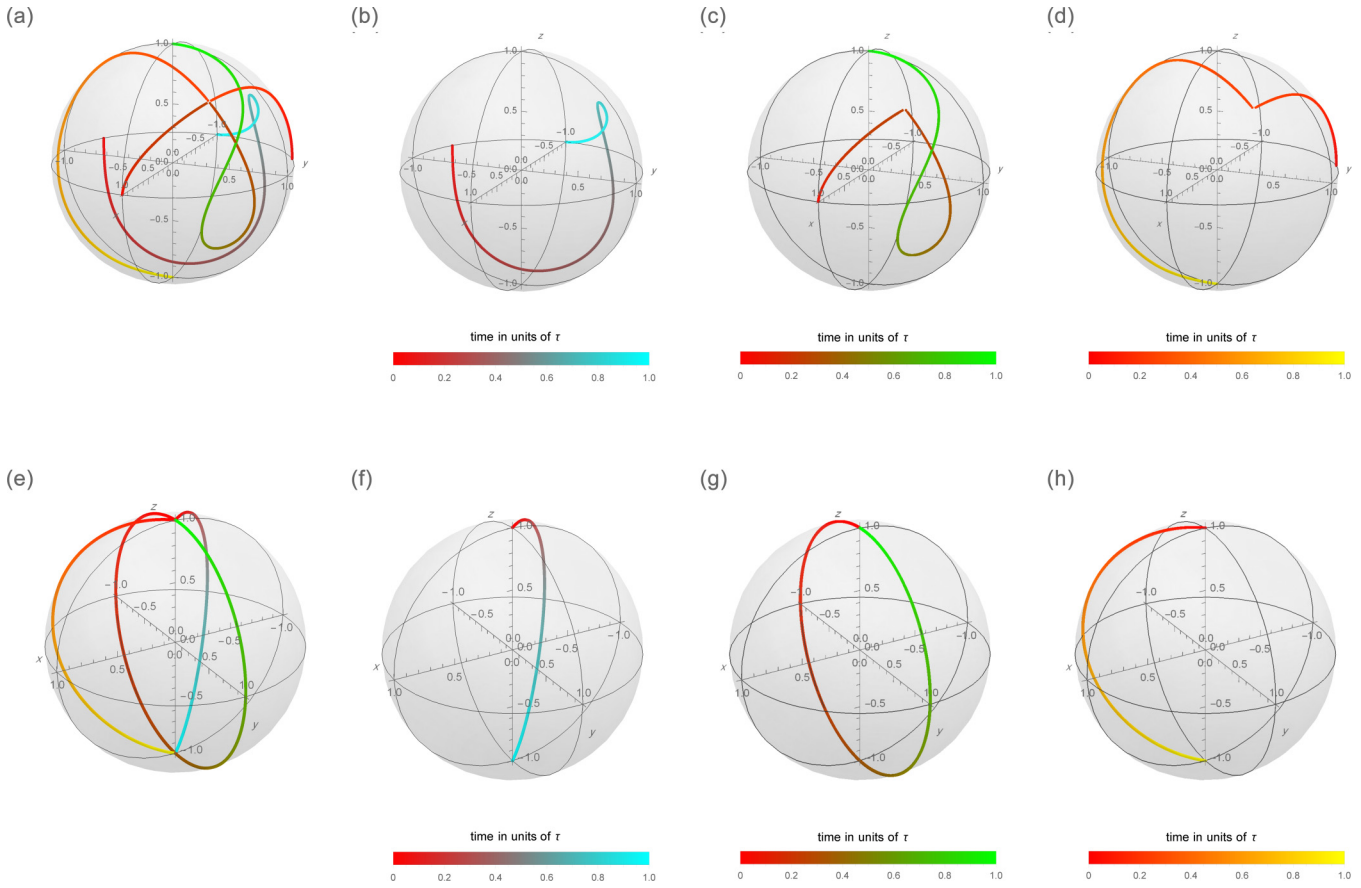

FIG. 3. Majorana sphere in the two frames of the four-level system: In the TP frame, we show the time evolution of (a) the Majorana sphere (all roots together); (b) the first root; (c) the second root; (d) the third root. We start with $|\psi\rangle = \frac{1}{\sqrt{2}}(|1\rangle + |4\rangle)$, which is represented by the three roots $z_1 = e^{-i\frac{2\pi}{3}}$, $z_2 = 1$, $z_3 = e^{i\frac{2\pi}{3}}$, and so by the three points $(\theta_1, \phi_1) = (\frac{\pi}{2}, -\frac{2\pi}{3})$, $(\theta_2, \phi_2) = (\frac{\pi}{2}, 0)$, $(\theta_3, \phi_3) = (\frac{\pi}{2}, \frac{2\pi}{3})$ on $\mathcal{S}^2$, and end with $|\psi\rangle \propto \frac{1}{\sqrt{2}}(|2\rangle - |3\rangle)$, which is represented by the two roots $z_1 = 0$, $z_2 = -1$, and so by the two points $(\theta_1, \phi_1) = (0, 0)$, $(\theta_2, \phi_2) = (\frac{\pi}{2}, \pi)$ on $\mathcal{S}^2$. In the laboratory frame, we show the time evolution on the Majorana sphere of (e) all the roots; (f) the first root; (g) the second root; (h) the third root. We start with $|\psi\rangle = |1\rangle$, which is represented by the three identical roots $z_1 = 0$, $z_2 = 0$, $z_3 = 0$, and so by the three identical points $(\theta_1, \phi_1) = (0, 0)$, $(\theta_2, \phi_2) = (0, 0)$, $(\theta_3, \phi_3) = (0, 0)$ on $\mathcal{S}^2$, and end with $|\psi\rangle \propto |3\rangle$, which is represented by the single root $z_1 = 0$, and so by the one point $(\theta_1, \phi_1) = (0, 0)$ on $\mathcal{S}^2$.

case, the representation is self-dual (the dual representation is isomorphic to to the representation itself), so that it is tempting to check what happens there with the retrograde canon scheme. Another tempting procedure to try to make is to derive a similar scheme for other self-dual groups, for which every irreducible representation is isomorphic to its dual.

The geometrical depiction that we presented gives rise to further questions for future study. We saw, for example, that we lose a root of the Majorana polynomial (in other words, the degree of the polynomial decreases by 1) when we arrive at the south pole. Another point is the peculiar behavior when two roots coalesce, namely that the trajectories feature sharp turns. We have here just a few example for this, but it might be an indicator of a more general phenomenon. A third observation is that when we run more numerical simulations for Pythagorean systems (four-level systems and 16-level systems, with different PTT and different k's), we always get the same circular trajectory which is the intersection between the y-z plane and the unit sphere (and other trajectories of other roots). This calls for an explanation.

We believe that our analytical schemes and our *natural maximally entangled bases* will offer a platform for quantum control and quantum information processing of multistate dynamics.

ACKNOWLEDGMENTS

We would like to thank A. Padan for useful discussions. M.G. gratefully acknowledges support by the Israel Science Foundation (Grant No. 227/15) and the US-Israel Binational Science Foundation (Grant No. 2016224). H.S. gratefully acknowledges support by the Israel Science foundation (Grant No. 1433/15) as well.

APPENDIX A: VECTORIZATION FUNCTION AND ITS INVERSE

Let X be an $m \times n$ matrix. $V(X)$ simply creates an mn-long column vector by stacking X's columns one after the other. We can define this more formally as follows. Let e_i denote the $n \times 1$ matrix (column vector) which is zero everywhere except

the ith component, which is 1 [in other words $(e_i)_{j1} = \delta_{ij}$]. Define E_i to be

$$E_i = e_i \otimes I_m. \tag{A1}$$

The vectorization function is then

$$V(X) = \sum_{i=1}^{n} E_i X e_i, \tag{A2}$$

and its inverse is

$$V^{-1}(Y) = \sum_{i=1}^{n} E_i^T Y e_i^T. \tag{A3}$$

A very useful property of this operator is

$$V(AXB) = (B^T \otimes A)V(X), \tag{A4}$$

and we use it frequently in this paper.

APPENDIX B: THE HAMILTONIAN OF THE 16-LEVEL SYSTEM IN THE TWO FRAMES

Here we present explicitly the 16-level system Hamiltonian in the two frames, the TP frame and the laboratory frame, as well as the symmetric orthogonal transformation matrix W that takes us from one basis to another:

$$H_{TP} = \begin{pmatrix}
3V_{14} & \sqrt{3}\Omega_2 & 0 & 0 & \sqrt{3}\Omega_1 & 0 & 0 & 0 & 0 & 0 & 0 & 0 & 0 & 0 & 0 & 0 \\
\sqrt{3}\Omega_2 & 3\Delta_1+\Delta_2 & 2\Omega_2 & 0 & 0 & \sqrt{3}\Omega_1 & 0 & 0 & 0 & 0 & 0 & 0 & 0 & 0 & 0 & 0 \\
0 & 2\Omega_2 & 3\Delta_1-\Delta_2 & \sqrt{3}\Omega_2 & 0 & 0 & \sqrt{3}\Omega_1 & 0 & 0 & 0 & 0 & 0 & 0 & 0 & 0 & 0 \\
0 & 0 & \sqrt{3}\Omega_2 & 3V_{23} & 0 & 0 & 0 & \sqrt{3}\Omega_1 & 0 & 0 & 0 & 0 & 0 & 0 & 0 & 0 \\
\sqrt{3}\Omega_1 & 0 & 0 & 0 & \Delta_1+3\Delta_2 & \sqrt{3}\Omega_2 & 0 & 0 & 2\Omega_1 & 0 & 0 & 0 & 0 & 0 & 0 & 0 \\
0 & \sqrt{3}\Omega_1 & 0 & 0 & \sqrt{3}\Omega_2 & V_{14} & 2\Omega_2 & 0 & 0 & 2\Omega_1 & 0 & 0 & 0 & 0 & 0 & 0 \\
0 & 0 & \sqrt{3}\Omega_1 & 0 & 0 & 2\Omega_2 & V_{23} & \sqrt{3}\Omega_2 & 0 & 0 & 2\Omega_1 & 0 & 0 & 0 & 0 & 0 \\
0 & 0 & 0 & \sqrt{3}\Omega_1 & 0 & 0 & \sqrt{3}\Omega_2 & \Delta_1-3\Delta_2 & 0 & 0 & 0 & 2\Omega_1 & 0 & 0 & 0 & 0 \\
0 & 0 & 0 & 0 & 2\Omega_1 & 0 & 0 & 0 & 3\Delta_2-\Delta_1 & \sqrt{3}\Omega_2 & 0 & 0 & \sqrt{3}\Omega_1 & 0 & 0 & 0 \\
0 & 0 & 0 & 0 & 0 & 2\Omega_1 & 0 & 0 & \sqrt{3}\Omega_2 & -V_{23} & 2\Omega_2 & 0 & 0 & \sqrt{3}\Omega_1 & 0 & 0 \\
0 & 0 & 0 & 0 & 0 & 0 & 2\Omega_1 & 0 & 0 & 2\Omega_2 & -V_{14} & \sqrt{3}\Omega_2 & 0 & 0 & \sqrt{3}\Omega_1 & 0 \\
0 & 0 & 0 & 0 & 0 & 0 & 0 & 2\Omega_1 & 0 & 0 & \sqrt{3}\Omega_2 & -\Delta_1-3\Delta_2 & 0 & 0 & 0 & \sqrt{3}\Omega_1 \\
0 & 0 & 0 & 0 & 0 & 0 & 0 & 0 & \sqrt{3}\Omega_1 & 0 & 0 & 0 & -3V_{23} & \sqrt{3}\Omega_2 & 0 & 0 \\
0 & 0 & 0 & 0 & 0 & 0 & 0 & 0 & 0 & \sqrt{3}\Omega_1 & 0 & 0 & \sqrt{3}\Omega_2 & \Delta_2-3\Delta_1 & 2\Omega_2 & 0 \\
0 & 0 & 0 & 0 & 0 & 0 & 0 & 0 & 0 & 0 & \sqrt{3}\Omega_1 & 0 & 0 & 2\Omega_2 & -3\Delta_1-\Delta_2 & \sqrt{3}\Omega_2 \\
0 & 0 & 0 & 0 & 0 & 0 & 0 & 0 & 0 & 0 & 0 & \sqrt{3}\Omega_1 & 0 & 0 & \sqrt{3}\Omega_2 & -3V_{14}
\end{pmatrix}, \tag{B1}$$

$$W_{16\times16} = \frac{1}{2}(\underline{00}, \underline{01}, \underline{10}, \underline{11}, \underline{31}, \underline{30}, \underline{21}, \underline{20}, \underline{23}, \underline{22}, \underline{33}, \underline{32}, \underline{12}, \underline{13}, \underline{02}, \underline{03})$$

$$= \frac{1}{2}\begin{pmatrix}
1 & 0 & 0 & 0 & 0 & 1 & 0 & 0 & 0 & 0 & 1 & 0 & 0 & 0 & 0 & 1 \\
0 & 1 & 0 & 0 & 1 & 0 & 0 & 0 & 0 & 0 & 0 & 1 & 0 & 0 & 1 & 0 \\
0 & 0 & 1 & 0 & 0 & 0 & 0 & 1 & 1 & 0 & 0 & 0 & 0 & 1 & 0 & 0 \\
0 & 0 & 0 & 1 & 0 & 0 & 1 & 0 & 0 & 1 & 0 & 0 & 1 & 0 & 0 & 0 \\
0 & 1 & 0 & 0 & 1 & 0 & 0 & 0 & 0 & 0 & 0 & -1 & 0 & 0 & -1 & 0 \\
1 & 0 & 0 & 0 & 0 & 1 & 0 & 0 & 0 & 0 & -1 & 0 & 0 & 0 & 0 & -1 \\
0 & 0 & 0 & 1 & 0 & 0 & 1 & 0 & 0 & -1 & 0 & 0 & -1 & 0 & 0 & 0 \\
0 & 0 & 1 & 0 & 0 & 0 & 0 & 1 & -1 & 0 & 0 & 0 & 0 & -1 & 0 & 0 \\
0 & 0 & 1 & 0 & 0 & 0 & 0 & -1 & -1 & 0 & 0 & 0 & 0 & 1 & 0 & 0 \\
0 & 0 & 0 & 1 & 0 & 0 & -1 & 0 & 0 & -1 & 0 & 0 & 1 & 0 & 0 & 0 \\
1 & 0 & 0 & 0 & 0 & -1 & 0 & 0 & 0 & 0 & -1 & 0 & 0 & 0 & 0 & 1 \\
0 & 1 & 0 & 0 & -1 & 0 & 0 & 0 & 0 & 0 & 0 & -1 & 0 & 0 & 1 & 0 \\
0 & 0 & 0 & 1 & 0 & 0 & -1 & 0 & 0 & 1 & 0 & 0 & -1 & 0 & 0 & 0 \\
0 & 0 & 1 & 0 & 0 & 0 & 0 & -1 & 1 & 0 & 0 & 0 & 0 & -1 & 0 & 0 \\
0 & 1 & 0 & 0 & -1 & 0 & 0 & 0 & 0 & 0 & 0 & 1 & 0 & 0 & -1 & 0 \\
1 & 0 & 0 & 0 & 0 & -1 & 0 & 0 & 0 & 0 & 1 & 0 & 0 & 0 & 0 & -1
\end{pmatrix}, \tag{B2}$$

$$H_{\text{Lab}} = \begin{pmatrix}
0 & \sqrt{3}V_{12} & 0 & V_{12} & 0 & 2V_{14} & 0 & 0 & 0 & -V_{12} & 0 & 0 & 0 & 0 & 0 & V_{14} \\
\sqrt{3}V_{12} & 0 & V_{12} & 0 & 2V_{14} & 0 & 0 & 0 & V_{34} & 0 & 0 & 0 & 0 & 0 & V_{23} & 0 \\
0 & V_{12} & 0 & \sqrt{3}V_{12} & 0 & 0 & 0 & 2V_{23} & 0 & 0 & 0 & V_{34} & 0 & V_{14} & 0 & 0 \\
V_{12} & 0 & \sqrt{3}V_{12} & 0 & 0 & 0 & 2V_{23} & 0 & 0 & 0 & -V_{12} & 0 & V_{23} & 0 & 0 & 0 \\
0 & 2V_{14} & 0 & 0 & 0 & \sqrt{3}V_{12} & 0 & V_{34} & 0 & 0 & 0 & V_{23} & 0 & V_{12} & 0 & 0 \\
2V_{14} & 0 & 0 & 0 & \sqrt{3}V_{12} & 0 & V_{34} & 0 & 0 & 0 & V_{14} & 0 & -V_{34} & 0 & 0 & 0 \\
0 & 0 & 0 & 2V_{23} & 0 & V_{34} & 0 & \sqrt{3}V_{12} & 0 & V_{23} & 0 & 0 & 0 & 0 & 0 & -V_{34} \\
0 & 0 & 2V_{23} & 0 & V_{34} & 0 & \sqrt{3}V_{12} & 0 & V_{14} & 0 & 0 & 0 & 0 & 0 & V_{12} & 0 \\
0 & V_{34} & 0 & 0 & 0 & 0 & 0 & V_{14} & 0 & \sqrt{3}V_{34} & 0 & V_{12} & 0 & 2V_{23} & 0 & 0 \\
-V_{12} & 0 & 0 & 0 & 0 & 0 & V_{23} & 0 & \sqrt{3}V_{34} & 0 & V_{12} & 0 & 2V_{23} & 0 & 0 & 0 \\
0 & 0 & 0 & -V_{12} & 0 & V_{14} & 0 & 0 & 0 & V_{12} & 0 & \sqrt{3}V_{34} & 0 & 0 & 0 & 2V_{14} \\
0 & 0 & V_{34} & 0 & V_{23} & 0 & 0 & 0 & V_{12} & 0 & \sqrt{3}V_{34} & 0 & 0 & 0 & 2V_{14} & 0 \\
0 & 0 & 0 & V_{23} & 0 & -V_{34} & 0 & 0 & 0 & 2V_{23} & 0 & 0 & 0 & \sqrt{3}V_{34} & 0 & V_{34} \\
0 & 0 & V_{14} & 0 & V_{12} & 0 & 0 & 0 & 2V_{23} & 0 & 0 & 0 & \sqrt{3}V_{34} & 0 & V_{34} & 0 \\
0 & V_{23} & 0 & 0 & 0 & 0 & 0 & V_{12} & 0 & 0 & 0 & 2V_{14} & 0 & V_{34} & 0 & \sqrt{3}V_{34} \\
V_{14} & 0 & 0 & 0 & 0 & 0 & -V_{34} & 0 & 0 & 0 & 2V_{14} & 0 & V_{34} & 0 & \sqrt{3}V_{34} & 0
\end{pmatrix}. \tag{B3}$$

APPENDIX C: THE TRANSFORMATION IN THE 64-LEVEL SYSTEM

For $N = 3$ (i.e., $n = 8$, that is, a 64-level system), we only write down explicitly the transformation matrix:

$$2\sqrt{2}\,W_{64\times 64} = \begin{matrix} (\underline{000}, & \underline{001}, & \underline{010}, & \underline{011}, & \underline{100}, & \underline{101}, & \underline{110}, & \underline{111}, \\ \underline{031}, & \underline{030}, & \underline{021}, & \underline{020}, & \underline{131}, & \underline{130}, & \underline{121}, & \underline{120}, \\ \underline{313}, & \underline{312}, & \underline{303}, & \underline{302}, & \underline{213}, & \underline{212}, & \underline{203}, & \underline{202}, \\ \underline{322}, & \underline{323}, & \underline{332}, & \underline{333}, & \underline{222}, & \underline{223}, & \underline{232}, & \underline{233}, \\ \underline{230}, & \underline{231}, & \underline{220}, & \underline{221}, & \underline{330}, & \underline{331}, & \underline{320}, & \underline{321}, \\ \underline{201}, & \underline{200}, & \underline{211}, & \underline{210}, & \underline{301}, & \underline{300}, & \underline{311}, & \underline{310}, \\ \underline{123}, & \underline{122}, & \underline{133}, & \underline{132}, & \underline{023}, & \underline{022}, & \underline{033}, & \underline{032}, \\ \underline{112}, & \underline{113}, & \underline{102}, & \underline{103}, & \underline{012}, & \underline{013}, & \underline{002}, & \underline{003}) \end{matrix} . \tag{C1}$$

APPENDIX D: THE MORE BASIC CPIs OF THE PYTHAGOREAN HAMILTONIAN

From the argument presented in Eq. (22) in the main text we can understand that there are more basic CPIs in our system, and from them we can build our universal CPI in any even-dimensional representation. Recall that the Hamiltonian

$$H(t) = \begin{cases} \Delta_1\sigma_z + \Omega_1\sigma_x, & 0 \leqslant t < \frac{T}{2}, \\ -\Delta_2\sigma_z - \Omega_2\sigma_x, & \frac{T}{2} \leqslant t \leqslant T \end{cases} \tag{D1}$$

has a propagator that satisfies

$$U(T,0) = (-1)^{\frac{p+q}{2}}\begin{pmatrix} 0 & 1 \\ -1 & 0 \end{pmatrix}, \tag{D2}$$

which means that in spin-$\frac{3}{2}$ representation, for example, we have

$$U(T,0) = (-1)^{\frac{p+q}{2}}\begin{pmatrix} 0 & 0 & 0 & 1 \\ 0 & 0 & -1 & 0 \\ 0 & 1 & 0 & 0 \\ -1 & 0 & 0 & 0 \end{pmatrix}. \tag{D3}$$

By our claims in the main text, the TP frame's 16×16 Hamiltonian (See Appendix B) fully transfers the state $\frac{1}{\sqrt{2}}(e_1 + e_{16})$ to another (orthogonal) state at $\frac{T}{2}$, and so does it for the initial state $\frac{1}{\sqrt{2}}(e_6 + e_{11})$. We will work now with tensor products in order to clarify how we obtain our previous CPI, and we assume, without loss of generality, that $(-1)^{\frac{p+q}{2}} = 1$.

According to the CPI scheme we derived in Eq. (24) in the main text, the (two independent) "basic" CPIs are

$$\frac{1}{\sqrt{2}}(|11\rangle + |44\rangle) \to \frac{1}{\sqrt{2}}U\left(\frac{T}{2},0\right)\otimes U\left(\frac{T}{2},0\right)(|41\rangle - |14\rangle), \tag{D4a}$$

$$\frac{1}{\sqrt{2}}(|33\rangle + |22\rangle) \to \frac{1}{\sqrt{2}}U\left(\frac{T}{2},0\right)\otimes U\left(\frac{T}{2},0\right)(|23\rangle - |32\rangle), \tag{D4b}$$

and both of them occur at $t = \frac{T}{2}$; and it is easy to see that our known CPI holds at $t = \frac{T}{2}$ too:

$$\begin{aligned} &\frac{1}{2}(|44\rangle + |33\rangle + |22\rangle + |11\rangle) \\ &\quad \to \frac{1}{2}U\left(\frac{T}{2},0\right)\otimes U\left(\frac{T}{2},0\right)(|41\rangle - |32\rangle + |23\rangle - |14\rangle) \\ &\quad = \frac{1}{2}(|41\rangle - |32\rangle + |23\rangle - |14\rangle), \end{aligned} \tag{D5}$$

where in the last step we used the fact that $uYu^T = Y$ (in every representation). We wrote this last CPI before in another way: $V(I_4) \to V(Y_4)$. What makes this CPI unique is that it is universal for every (even) representation, while the "basic" CPIs we have just seen are not. It is easy to see that for every $|\psi_0(\alpha,\beta)\rangle = \frac{\alpha}{\sqrt{2}}(|11\rangle + |44\rangle) + \frac{\beta}{\sqrt{2}}(|33\rangle + |22\rangle)$ we have a CPI ($|\alpha|^2 + |\beta|^2 = 1$), since the basic CPI's initial and final states are built of different (and orthogonal) one-particle states, so that the final state (at $t = \frac{T}{2}$) we get from propagating $|\psi_0(\alpha,\beta)\rangle$ is orthogonal, by definition, to the initial state. But, as we have mentioned, with $\alpha = \beta = \frac{1}{2}$ we have a universal CPI.

For a general even representation n, we have $\frac{n}{2}$ basic CPIs of the form ($i \in \{1, 2, \ldots, \frac{n}{2}\}$)

$$\begin{aligned} &\frac{1}{\sqrt{2}}(|ii\rangle + |n+1-i, n+1-i\rangle) \\ &\quad \to (-1)^i\frac{1}{\sqrt{2}}U\left(\frac{T}{2},0\right)\otimes U\left(\frac{T}{2},0\right) \\ &\qquad (|i, n+1-i\rangle - |n+1-i, i\rangle), \end{aligned} \tag{D6}$$

which are to be calculated in that representation. However, as we have discussed, the sum of all these states exhibits a known CPI, which is independent of the parameters p, q, k:

$$\frac{1}{\sqrt{n}}\sum_{i=1}^{n}|ii\rangle \to \frac{1}{\sqrt{n}}\sum_{i=1}^{n}(-1)^i|i, n+1-i\rangle, \tag{D7}$$

which is absolutely the known one.

APPENDIX E: THE ISSUE IN ODD-DIMENSIONAL REPRESENTATIONS

From Eq. (24) in the main text and Appendix D, one can clearly see the issue in odd-dimensional representations we discussed in the main text from another point of view. For

simplicity we will demonstrate the problem in the three-level system of spin-1 representation. Assuming that $U(T,0)=Y$, we get in the spin-1 representation

$$U(T,0)=\begin{pmatrix}0&0&1\\0&-1&0\\1&0&0\end{pmatrix},$$

which means

$$U(T,0)|1\rangle = |3\rangle, \tag{E1a}$$
$$U(T,0)|2\rangle = -|2\rangle, \tag{E1b}$$
$$U(T,0)|3\rangle = |1\rangle. \tag{E1c}$$

According to Eq. (24) in the main text, this guarantees just one CPI in the retrograde canon's TP frame Hamiltonian, $\mathcal{H}(t)=-H(T-t)\otimes I + I\otimes H(t)$:

$$\begin{aligned}&\frac{1}{\sqrt{2}}(-|11\rangle+|33\rangle)\\&\quad\to\frac{1}{\sqrt{2}}U\left(\frac{T}{2},0\right)\otimes U\left(\frac{T}{2},0\right)(-|31\rangle+|13\rangle)\\&\quad\text{at } t=\frac{T}{2},\end{aligned} \tag{E2}$$

which is obviously not universal and does depend on more details of $H(t)$, just like the other analogous "basic" CPIs we have seen in even representations. So we do not have a similar picture that allows us to repeat the same way to build a universal CPI. It does hold that if we start with $V(I)$ we end in $V(Y)$ at $t=\frac{T}{2}$, but we cannot see this directly from Eq. (24) in the main text as we did in even representations, and, in any case, this is not a CPI since the two states are not orthogonal.

APPENDIX F: THE MAJORANA SPHERE

According to Majorana's representation, there is a one-to-one correspondence between the (normalized) states of an N-level system, which are of the form

$$|\psi\rangle = \sum_{k=1}^{N} c_k|k\rangle \tag{F1}$$

(where $\sum_{k=1}^{N}|c_k|^2=1$), and the (normalized) $N-1$ Majorana polynomials, which are of the form

$$M(z)=\sum_{k=1}^{N} d_k\binom{N-1}{k-1}^{\frac{1}{2}}(-z)^{N-k} \tag{F2}$$

(where $\sum_{k=1}^{N}|d_k|^2=1$). This bijection is given trivially by [41–43]

$$d_k = c_k \quad \forall\, k. \tag{F3}$$

Every polynomial of this form is defined, up to a phase, by its roots, whose number can be $N-1$ (when $c_1\neq 0$), $N-2$ (when $c_1=0$ and $c_2\neq 0$), $N-3$ (when $c_1=0$ and $c_2=0$ and $c_3\neq 0$), etc. Hence, there is a map from the set of these polynomials to the set $\mathcal{C}_N$,

$$\mathcal{C}_N = \{\,\}\cup\bigcup_{k=1}^{N-1}\mathbb{C}^k, \tag{F4}$$

and every element in $\mathcal{C}_N$ uniquely corresponds to a state $|\psi\rangle$, up to a phase (the empty set corresponds to $|\psi\rangle=|N\rangle$ up to a phase). Now, every root z can be presented on the unit sphere (also the Riemann sphere or the Bloch sphere or the Majorana sphere in this context) $\mathcal{S}^2$ by using the stereographic projection from the south pole [44]:

$$z=\tan\frac{\theta}{2}e^{i\phi}, \tag{F5a}$$
$$\theta = 2\arctan|z|, \tag{F5b}$$
$$\phi = -i\ln\frac{z}{|z|}. \tag{F5c}$$

Therefore, when we discuss an N-level system, we can describe its state (up to a phase) by a Majorana sphere with 0 or 1 or 2 or ... or $N-1$ points on it. Majorana's theorem states that, with an applied magnetic field on the system (which has angular momentum j, where $N=2j+1$ and $|k\rangle$ in our notation is $|j,m=k-j\rangle$), these representative points precess rigidly around the direction of the field.

Generally, in an N-level system, the time evolution on the Majorana sphere can be represented by $N-1$ trajectories, where each trajectory describes the evolution of one of the roots, and trajectories may intersect for some values of time. If at some time there are $0\leqslant n\leqslant N-1$ points on the Majorana sphere, this means that the polynomial is of degree i for some $n\leqslant i\leqslant N-1$, which implies that $c_1, c_2, \ldots, c_{N-1-i}$ are zero. This hold of course for an interval of time as well.

[1] D. D'Alessandro, *Introduction to Quantum Control and Dynamics*, 1st ed. (Taylor & Francis, Hoboken, NJ, 2007).

[2] B. P. Lanyon, M. Barbieri, M. P. Almeida, T. Jennewein, T. C. Ralph, K. J. Resch, G. J. Pryde, J. L. O'Brien, A. Gilchrist, and A. G. White, Simplifying quantum logic using higher-dimensional hilbert spaces, Nat. Phys. **5**, 134 (2008).

[3] N. J. Cerf, M. Bourennane, A. Karlsson, and N. Gisin, Security of Quantum Key Distribution Using d-Level Systems, Phys. Rev. Lett. **88**, 127902 (2002).

[4] M. A. Nielsen and I. L. Chuang, *Quantum Computation and Quantum Information: 10th Anniversary Edition* (Cambridge University Press, Cambridge, 2010).

[5] D. M. Reich, N. Katz, and C. P. Koch, Exploiting non-Markovianity for quantum control, Sci. Rep. **5**, 12430 (2015).

[6] G. Alzetta, A. Gozzini, L. Moi, and G. Orriols, An experimental method for the observation of r.f. transitions and laser beat resonances in oriented Na vapour, Nuovo Cimento B **36**, 5 (1976).

[7] J. Keeler, *Understanding NMR Spectroscopy*, 2nd ed. (Wiley, New York, 2011).

[8] A. Stolow, Applications of wavepacket methodology, Philos. Trans. R. Soc. A **356**, 345 (1998).

[9] C. Slichter, *Principles of Magnetic Resonance*, Springer Series in Solid-State Sciences (Springer, Berlin, 1990).

[10] J. I. Cirac, P. Zoller, H. J. Kimble, and H. Mabuchi, Quantum State Transfer and Entanglement Distribution among Distant Nodes in a Quantum Network, Phys. Rev. Lett. **78**, 3221 (1997).

[11] D. Bouwmeester, A. Ekert, and A. Zeilinger, *The Physics of Quantum Information: Quantum Cryptography, Quantum Teleportation, Quantum Computation* (Springer, Berlin, 2013).

[12] W. S. Warren, H. Rabitz, and M. Dahleh, Coherent control of quantum dynamics: The dream is alive, Science **259**, 1581 (1993).

[13] L. Allen and J. Eberly, *Optical Resonance and Two-level Atoms*, Dover Books on Physics and Chemistry (Dover, Mineola, NY, 1987).

[14] B. T. Torosov and N. V. Vitanov, Exactly soluble two-state quantum models with linear couplings, J. Phys. A: Math. Theor. **41**, 155309 (2008).

[15] G. Turinici and H. Rabitz, Quantum wavefunction controllability, Chem. Phys. **267**, 1 (2001).

[16] A. J. Pounds, Introduction to quantum mechanics: A time-dependent perspective (David J. Tannor), J. Chem. Educ. **85**, 919 (2008).

[17] G. T. Genov, B. T. Torosov, and N. V. Vitanov, Optimized control of multistate quantum systems by composite pulse sequences, Phys. Rev. A **84**, 063413 (2011).

[18] I. R. Solá, V. S. Malinovsky, and D. J. Tannor, Optimal pulse sequences for population transfer in multilevel systems, Phys. Rev. A **60**, 3081 (1999).

[19] J. R. Kuklinski, U. Gaubatz, F. T. Hioe, and K. Bergmann, Adiabatic population transfer in a three-level system driven by delayed laser pulses, Phys. Rev. A **40**, 6741 (1989).

[20] V. Paulisch, H. Rui, H. K. Ng, and B.-G. Englert, Beyond adiabatic elimination: A hierarchy of approximations for multiphoton processes, Eur. Phys. J. Plus **129**, 12 (2014).

[21] F. T. Hioe, N-level quantum systems with SU(2) dynamic symmetry, J. Opt. Soc. Am. B **4**, 1327 (1987).

[22] A. A. Rangelov and N. V. Vitanov, Complete population transfer in a three-state quantum system by a train of pairs of coincident pulses, Phys. Rev. A **85**, 043407 (2012).

[23] K. Y. Rakhimov, K. K. Shakov, and J. H. McGuire, Complete population transfer in a degenerate three-state atom, Phys. Rev. A **69**, 023405 (2003).

[24] J. Gong and S. Rice, Complete quantum control of the population transfer branching ratio between two degenerate target states, J. Chem. Phys. **121**, 1364 (2004).

[25] S. Carrasco, J. Rogan, and J. A. Valdivia, Speeding up maximum population transfer in periodically driven multi-level quantum systems, Sci. Rep. **9**, 16270 (2019).

[26] E. A. Shapiro, V. Milner, and M. Shapiro, Complete transfer of populations from a single state to a preselected superposition of states using piecewise adiabatic passage: Theory, Phys. Rev. A **79**, 023422 (2009).

[27] S. Zhdanovich, E. A. Shapiro, J. W. Hepburn, M. Shapiro, and V. Milner, Complete transfer of populations from a single state to a pre-selected superposition of states using piecewise adiabatic passage: Experiment, Phys. Rev. A **80**, 063405 (2009).

[28] H. Suchowski, Y. Silberberg, and D. B. Uskov, Pythagorean coupling: Complete population transfer in a four-state system, Phys. Rev. A **84**, 013414 (2011).

[29] E. Svetitsky, H. Suchowski, R. Resh, Y. Shalibo, J. M. Martinis, and N. Katz, Hidden two-qubit dynamics of a four-level Josephson circuit, Nat. Commun. **5**, 5617 (2014).

[30] A. Padan and H. Suchowski, A quantum retrograde canon: complete population inversion in n^2-state systems, New J. Phys. **20**, 043021 (2018).

[31] N. V. Vitanov, T. Halfmann, B. W. Shore, and K. Bergmann, Laser-induced population transfer by adiabatic passage techniques, Annu. Rev. Phys. Chem. **52**, 763 (2001).

[32] N. Kumar, K. Chaitanya, and B. Bambah, Quantum entanglement in coupled lossy waveguides using SU(2) and SU(1, 1) thermo-algebras, J. Mod. Phys. **06**, 1554 (2015).

[33] T. L. Curtright, D. B Fairlie, and C. K. Zachos, A compact formula for rotations as spin matrix polynomials, SIGMA. Symmetry, Integrability and Geometry: Methods and Applications **10**, 084 (2014).

[34] T. Curtright, More on rotations as spin matrix polynomials, J. Math. Phys. **56**, 091703 (2015).

[35] H. Poincaré, Sur le probléme des trois corps et les équations de la dynamique, Acta Math. **13**, 1 (1890).

[36] H. Poincaré, Sur le probléme des trois corps et les équations de la dynamique, Oeuvres **VII**, 262 (theorem 1 section 8).

[37] C. Carathéodory, Über den Wiederkehrsatz von Poincaré, Berl. Sitzungsber, 580 (1919).

[38] C. Carathéodory, Über den Wiederkehrsatz von Poincaré, Ges. Math. Schr. **IV**, 296 (1919).

[39] F. Bloch, Nuclear induction, Phys. Rev. **70**, 460 (1946).

[40] M. Born, E. Wolf, A. B. Bhatia, P. C. Clemmow, D. Gabor, A. R. Stokes, A. M. Taylor, P. A. Wayman, and W. L. Wilcock, *Principles of Optics: Electromagnetic Theory of Propagation, Interference and Diffraction of Light*, 7th ed. (Cambridge University Press, Cambridge, 1999).

[41] E. Majorana, Atomi orientati in campo magnetico variabile, Nuovo Cimento (1924–1942) **9**, 43 (1932).

[42] E. Majorana and M. Inguscio, Oriented atoms in a variable magnetic field, in *Ettore Majorana Scientific Papers: On Occasion of the Centenary of his Birth*, edited by G. F. Bassani (Springer, Berlin, 2006), pp. 113–136.

[43] F. Bloch and I. I. Rabi, Atoms in variable magnetic fields, Rev. Mod. Phys. **17**, 237 (1945).

[44] M. R. Dennis, Canonical representation of spherical functions: Sylvester's theorem, Maxwell's multipoles and Majorana's sphere, J. Phys. A: Math. Gen. **37**, 9487 (2004).

[45] B. Hall, *Quantum Theory for Mathematicians*, Graduate Texts in Mathematics (Springer, New York, 2013), Chap. 18.

[46] J. Wang, F. Sciarrino, A. Laing, and M. G. Thompson, Integrated photonic quantum technologies, Nat. Photon. **14**, 273 (2020).

[47] K. Mølmer and A. Sørensen, Multiparticle Entanglement of Hot Trapped Ions, Phys. Rev. Lett. **82**, 1835 (1999).